that produces no interference to the passage of the full-energy ion component.

The critical problem of our future experiments is to optimize the interface between the gas cell exit, the transverse magnetic field, and the ground potential geometry. Two types of electron power drain are possible from this interface region. First, electron leakage may occur from the gas cell; we have controlled this in the present geometry. Second, opening the gas cell to permit passage of the entire unneutralized beam will permit one-half- and one-third-energy ions to strike the outside surface of the gas cell. Secondary electrons emitted from this region will be an additional power drain that must be controlled.

This reseach was sponsored by the Office of Fusion Energy (ETM), U.S. Department of Energy under Contract No. W-7405-eng-26 with the Union Carbide Corporation.

[1]W.L. Barr and R.W. Moir, Proc. 2nd Topical Meeting on Technology of Controlled Nuclear Fusion, 1976, Vol. IV, p. 1181; W.L. Barr, J.N. Doggett, G.W. Hamilton, J.D. Kinney, and R.W. Moir, Proc. 7th Symp. on Engineering Problems of Fusion Research, 1978, Vol. I, p. 308.
[2]P. Raimbault, EUR-CEA-FC-823, 1976.
[3]G.G. Kelley and O.B. Morgan, Phys. Fluids **4**, 1446 (1961).
[4]W.L. Stirling, C.C. Tsai, H.H. Haselton, D.E. Schechter, J.H. Whealton, W.K. Dagenhart, R.C. Davis, W.L. Gardner, M.M. Menon, and P.M. Ryan, Rev. Sci. Instrum. **50**, 523 (1979).

Observations consistent with self-generated magnetic fields in CO_2 laser-produced plasmas

N. A. Ebrahim, M. C. Richardson, and R. Fedosejevs
National Research Council of Canada, Division of Physics, Ottawa, K1A 0R6, Canada

U. Feldman
E.O. Hulburt Center for Space Research, Naval Research Laboratory, Washington, D.C. 20375

(Received 16 March 1979; accepted for publication 11 May 1979)

The spatial structure of extreme ultraviolet (XUV) line emission from plasmas produced by nanosecond CO_2 laser pulses has been examined with a slitless normal-incidence vacuum-ultraviolet spectrograph in the 200–500-Å spectral region. The anomalous structural behavior of these spectra is consistent with the existence of self-generated magnetic fields. These fields could also explain the gross plasma structure observed through picosecond interferometry.

PACS numbers: 52.50.Jm, 52.35.Fp

Monochromatic two-dimensional imaging techniques in the extreme ultraviolet (xuv) provide a powerful diagnostic of the characteristics of multiply charged ions in high-density plasmas. Employed in the investigations of laser-produced plasmas, they enable the imaging of the plasma in the individual line radiation of specific ions.[1–3] In this communication we wish to report some unusual features in the images of the plasma plume produced off plane targets by intense nanosecond CO_2 radiation, observed with the aid of an xuv spectroheliograph. In particular, it is suggested that their interpretation is consistent with the existence of magnetic fields within these plasma. Such fields may also explain the anomalous structure observed in picosecond interferograms.

The relevance of self-generated magnetic fields to laser fusion studies lies in their possible effects on absorption efficiency, hydrodynamic motion, and thermal transport. Such fields have been the subject of experimental investigation for some time,[4] and recent optical probe measurements have confirmed their existence in plasma produced by intense 1-μm laser pulses.[5,6] However, because Faraday rotation diagnosis of magnetic fields is dependent on the plasma density, measurements of B fields in the region of the critical density of CO_2 laser-produced plasmas are limited in sensitivity to fields $\geqslant 1$ MG. The present studies suggest that self-generated magnetic fields strongly influence the dynamics of the expanding plasma.

The experimental arrangement is shown in Fig. 1. Flat massive targets are illuminated by the output of the COCO-II laser system [35 J, 1.5 ns (FWHM)] focused to a half-energy diameter of 110 μm with $f/2.5$ off-axis parabolic optics[7] providing peak intensities of 2×10^4 W/cm^2. Spectra of emission from the plasma were studied using the slitless

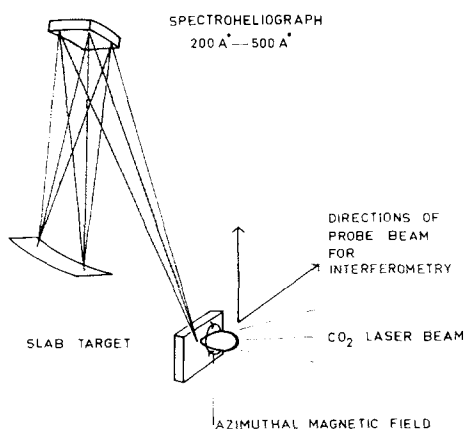

FIG. 1. Schematic of experimental arrangement.

 0003-6951/79/020106-03$00.50

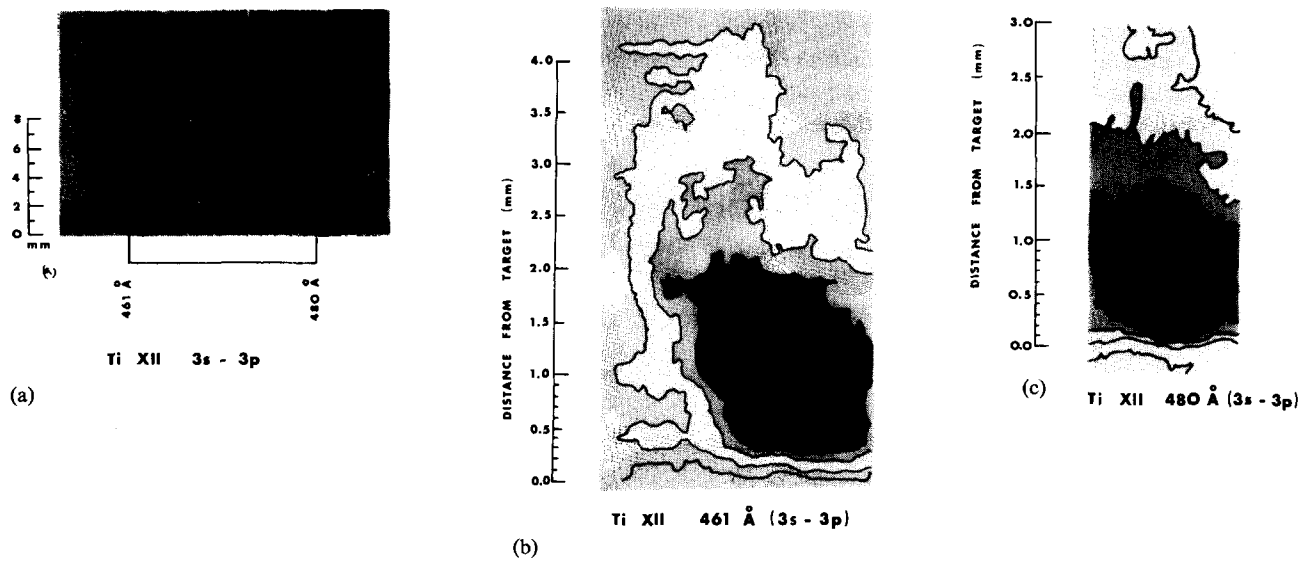

FIG. 2. (a) XUV image of Ti XII 3*s*-3*p* 461 and 480-Å transitions. The isodensity contour plots of these two transitions are shown in (b) and (c), respectively. The shadings indicate areas of equal photographic density, black corresponding to the highest density.

XUV spectrograph (spectroheliograph) described in Ref. 1, operating in the 200–500-Å spectral range. The spectroheliograph produces image of the plasma in discrete XUV emission lines, which are recorded on film and are therefore time averaged over the plasma lifetime. For these experiments the source grating distance was 165 cm and the grating film distance was 72 cm, giving a magnification of 0.43 and a reciprocal dispersion at the film plane of 3.89 Å/mm. The astigmatic blur in the focal plane along the direction of plasma expansion, at about 300 Å, is less than 22 μm, and this determines the spatial resolution in this direction. Thus, the spatial resolution is 22/0.43 μm$\simeq$50 μm. In the direction of dispersion the blur is 10 μm, and this limits the spatial resolution in this direction to 10/0.43 μm$\simeq$23 μm.

Figure 2(a) shows the XUV images of the emission from Ti XII 3*s*-3*p* transitions at 461 and 480 Å. The continuous emission close to the target surface is free-free and free-bound continuum. Normal to the target surface the resolution is purely spatial, while parallel to the target surface the resolution is both spatial and spectral. The contribution of thermal-ion Doppler broadening to the image size, for $T_e \simeq 400$ eV and $\lambda = 461$ Å, is $\Delta\lambda_D = \lambda/c(2kT_e/M)^{1/2} = 0.1$ Å, which corresponds to about 60 μm at the target surface. Doppler broadening due to the expansion velocity can be expressed as $\Delta\lambda = (\lambda v \sin\alpha)/c$, where v is the average expansion velocity and α is the half-angle of the expanding plume. Assuming $v \sim 2\times 10^7$ cm/s and $\alpha \sim 15°$, $\Delta\lambda = 0.08$ Å, which corresponds to about 50 μm at the target surface, although, in general, α is less than 15° in these experiments. Thus, the resulting spectral image quite accurately portrays the shape of the plasma in both directions. For these experiments the target normal was tilted 35° to the incoming laser beam direction. In Figs. 2(b) and 2(c), two-dimensional photographic isodensity contour plots of the two distributions in Fig. 2(a) are shown. The target surface is defined by the edge of the continuum emission. The images of Ti XII emission from the plasma are of interest in that they appear as narrow collimated cylindrical structures having diameters between 500 and 700 μm, the emission being observed up to about 8 mm from the target surface. Thus, they imply that the highly ionized plasma blowoff is extremely directional, with the cylinder axis being parallel to the incoming pulse. In some of the spectra, however, there is evidence that two separate structures may be present. One cylindrical structure expands in the direction of the incoming pulse while the second structure, also a cylinder, expands at an angle closer to the target normal. Rather similar behavior to this is observed in images of Al IX and Al X emission from plasmas produced off aluminum targets. However, in both cases images of the emission from the low-ionization stages (e.g., Ti VII and Al VII) have a much smaller spatial extent and appear as brighter regions in the continuum. The emission from the lower-ionization stages in both cases does not appear to be as sharply collimated as is the case with the higher-ionization stages. These ions are probably formed as a result of recombination from higher-ionization stages, and exist in the cool-

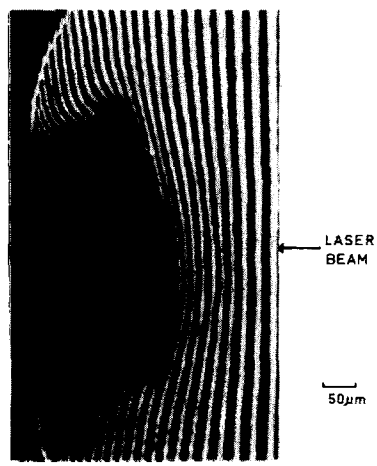

FIG. 3. Picosecond interferogram of plasma produced off $(CH_2)_n$ target by a 30-J CO_2 pulse taken at a time of 4.1 ns after the leading edge of the CO_2 laser pulse.

er plasma at much later times after the laser pulse. The prominent features obtained in this spectral regions from polyethylene plasma emission are the CIV images which are also probably formed as a result of recombination in the late-time cooler plasma.

The spatial structure of the plasma has also been studied by means of picosecond interferometry using a 100-ps 0.53-μm probe pulse.[8] It is found that ponderomotive effects give rise to steep density gradients $\sim 10\,\mu$m in the region of the critical surface during the laser pulse. In addition, simultaneous interferometry in two orthogonal directions indicates a complex structure with rippling and cratering of the critical density surface.[9] Immediately after the laser pulse, the morphology of the plasma becomes clearer as it expands into vacuum. In the case of plasma produced on polyethylene targets, a cylindrically confined expansion is observed. An interferogram of such a plasma taken at a time of 4.1 ns after the leading edge of the CO_2 laser pulse is shown in Fig. 3. A complete sequence of interferograms shows that at early times the plasma tends to be cylindrical in shape with sharp boundaries defined by abrupt changes in the fringe shift. After a time of 8–10 ns the cylindrical structure disperses as the leading edge of the profile spreads radially. The beginning of this transverse expansion is visible in Fig. 3.

It is possible to explain these effects in terms of the existence of large-scale azimuthal self-generated magnetic fields. Defining the ratio of the plasma pressure to the magnetic pressure conventionally as $\beta = 2\mu_0 nkT_e/B^2$, it is clear that MHD effects will directly influence the plasma dynamics in the regions where $\beta < 1$. Thus, we can expect the magnetic pressure to play a significant role in the hydrodynamics of the underdense plasma, for values of B which are not excessively high. In the critical region for $n = 10^{19}$ cm^{-3}, temperatures of 400 eV have been measured from x-ray line ratios,[10] resulting in $\beta = 1$ for $B \simeq 400$ kG. After the laser pulse, as the plasma expands and cools, fields of several hundred kilogauss could confine densities of several times 10^{19} cm^{-3}. In the underdense region, approximately 1 mm from the target surface where $n = 2\times 10^{18}$ cm^{-3} and $T_e \simeq 100$ eV, as deduced from the spectroheliograms,[3] $\beta = 1$ for $B \simeq 100$ kG.

Numerous mechanisms exist for the generation of fields of this magnitude,[4] the most common being the macroscopic $\nabla n \times \nabla T_e$ generating term. Although for CO_2 laser-produced plasma the growth rate for the magnetic field can be high, the maximum field values are limited by saturation mechanisms. For example, we can estimate the field growth rate from Max, Manheimer, and Thomson[11] as

$$\frac{\Delta B}{1\ \text{MG}} \simeq 10\left(\frac{\Delta t}{100\ \text{ps}}\right)\left(\frac{T_e}{1\ \text{keV}}\right)\left(\frac{10\ \mu\text{m}}{L}\right)^2 \sin\theta\,.$$

Taking $L \sim 50\,\mu$m, for orthogonal temperature and density gradients, gives $\dot{B} \sim 160$ kG/100 ps, for $T_e \sim 400$ eV. However, a crude estimate taking into account the saturation of the field yields magnitudes of[11]

$$B_s \simeq 3.6\left(\frac{T_e}{1\ \text{keV}}\right)^{1/2}\left(\frac{10\ \mu\text{m}}{L}\right)\left(\frac{A}{Z+1}\right)^{1/2} = 600\ \text{kG}$$

under the same conditions. Such magnetic fields would be high enough to confine the expanding plasma and would explain the gross features obtained in both the XUV spectra and the optical inteferograms.

[1] U. Feldman, G.A. Doschek, D.K. Prinz, and D.J. Nagel, J. Appl. Phys. **47**, 1341 (1976).
[2] G.A. Doschek, U. Feldman, P.G. Burkhalter, T. Finn, and W.A. Feibelman, J. Phys. B **10**, L745 (1977).
[3] N.A. Ebrahim, U. Feldman, G.A. Doschek, M.C. Richardson, and G.D. Enright, Bull. Am. Phys. Soc. **23**, 838 (1978).
[4] For a comprehensive bibliography of previous experimental investigations of self-generated magnetic fields in laser produced plasmas see J.A. Stamper, NRL Report 3872, 1978.
[5] J.A. Stamper, E.A. McLean, and B.H. Ripin, Phys. Rev. Lett. **40**, 1177 (1978).
[6] A. Raven, O. Willi, and P.T. Rumsby, Phys. Rev. Lett. **41**, 554 (1978).
[7] M.C. Richardson, N.H. Burnett, H.A. Baldis, G.D. Enright, R. Fedosejevs, N.R. Isenor, and I.V. Tomov, *Laser Interaction and Related Plasma Phenomena*, edited by H.J. Schwarz and H. Hora (Plenum, New York, 1977), Vol. 4A, p. 161.
[8] R. Fedosejevs, I.V. Tomov, N.H. Burnett, G.D. Enright, and M.C. Richardson, Phys. Rev. Lett. **39**, 932 (1977).
[9] R. Fedosejevs, M.D.J. Burgess, G.D. Enright, and M.C. Richardson, Bull. Am. Phys. Soc. **23**, 768 (1978).
[10] G.D. Enright, N.H. Burnett, and M.C. Richardson, Appl. Phys. Lett. **31**, 494 (1977).
[11] C.E. Max, W.M. Manheimer, and J.J. Thomson, Phys. Fluids **21**, 128 (1978).